

---

# BigVGAN: A Universal Neural Vocoder with Large-Scale Training

---

Sang-gil Lee<sup>1\*</sup> Wei Ping<sup>2†</sup> Boris Ginsburg<sup>2</sup>  
Bryan Catanzaro<sup>2</sup> Sungroh Yoon<sup>1,3†</sup>

<sup>1</sup>Data Science & AI Lab., Seoul National University (SNU)

<sup>2</sup>NVIDIA

<sup>3</sup>AIIS, ASRI, INMC, ISRC, NSI, and Interdisciplinary Program in AI, SNU

tkdr1f9202@snu.ac.kr wping@nvidia.com bginsburg@nvidia.com  
bcatanzaro@nvidia.com sryoon@snu.ac.kr

## Abstract

Despite recent progress in generative adversarial network (GAN)-based vocoders, where the model generates raw waveform conditioned on mel spectrogram, it is still challenging to synthesize high-fidelity audio for numerous speakers across varied recording environments. In this work, we present BigVGAN, a universal vocoder that generalizes well under various unseen conditions in zero-shot setting. We introduce periodic nonlinearities and anti-aliased representation into the generator, which brings the desired inductive bias for waveform synthesis and significantly improves audio quality. Based on our improved generator and the state-of-the-art discriminators, we train our GAN vocoder at the largest scale up to 112M parameters, which is unprecedented in the literature. In particular, we identify and address the training instabilities specific to such scale, while maintaining high-fidelity output without over-regularization. Our BigVGAN achieves the state-of-the-art zero-shot performance for various out-of-distribution scenarios, including new speakers, novel languages, singing voices, music and instrumental audio in unseen (even noisy) recording environments.<sup>3</sup> We will release our code and model at: <https://github.com/NVIDIA/BigVGAN>.

## 1 Introduction

Deep generative models have demonstrated noticeable successes for modeling raw audio. The successful methods include, autoregressive models [52, 30, 15], flow-based models [53, 38, 42, 18, 40, 25], GAN-based models [22, 3, 56, 19], and diffusion models [20, 6, 24].

Among these methods, GAN-based vocoders [e.g., 19] can generate high-fidelity raw audio conditioned on mel spectrogram, while synthesizing hundreds of times faster than real-time on a single GPU. However, existing GAN vocoders are confined to the settings with a moderate number of voices recorded in clean environment due to the limited model capacity. The audio quality can heavily degrade when the models are conditioned on mel spectrogram from unseen speakers in different recording environments. In practice, a universal vocoder, that can do zero-shot generation for out-of-distribution samples, is very valuable in many applications, including text-to-speech with numerous

---

\*Work done during an internship at NVIDIA.

†Corresponding authors.

<sup>3</sup>Listen to audio samples from BigVGAN at: <https://bigvgan-demo.github.io/>.

speakers [39], neural voice cloning [2, 13], voice conversion [26], speech-to-speech translation [12], and neural audio codec [59], where the studio-quality recordings are often not available.

Scaling up the model for zero-shot conditional generation is a noticeable trend in text generation [e.g., 5] and image synthesis [e.g., 45], but has not been explored in audio synthesis. Although likelihood-based models are found to be easy for scaling because of the simple training objective and stable optimization, we build our universal vocoder with large scale GAN training, because GAN vocoders have the following advantages: *i*) In contrast to autoregressive or diffusion models, it is fully parallel and requires only one forward pass to generate high-dimensional waveform.<sup>4</sup> *ii*) It does not impose any architectural constraints compared with flow-based models, which needs to keep the bijection between latents and data (see analysis in [40]). This architectural flexibility can lead to large model capacity when we scale up the size of the generator.

In this work, we present BigVGAN, a big vocoding GAN that enables high-fidelity zero-shot generation. We achieve this goal by improving the generator architecture and scaling it up to unprecedented size. Specifically, we make the following contributions:

1. We introduce periodic activations into the generator network, which provides the desired inductive bias for audio synthesis because waveforms exhibit high periodicity. In addition, we use the filtered nonlinearities within every convolutional layer for anti-aliasing purposes, which can further reduce the high-frequency artifacts within the synthesized waveform.
2. We combine our improved generator with the state-of-the-art discriminators. We demonstrate that our BigVGAN-base with 14M parameters outperforms the state-of-the-art HiFi-GAN vocoder with the same size, especially for unseen recording conditions and out-of-distribution samples.
3. We scale BigVGAN up to 112M parameters and train it on the entire LibriTTS dataset [60]. We address the training instabilities specific to such scale, while maintaining high-fidelity output without over regularizing both generator and discriminators. Our BigVGAN outperforms the state-of-the-art methods by a large margin for zero-shot generation at various out-of-distribution scenarios, including unseen speakers, novel languages, singing voices, music and instrumental audio in varied unseen recording environments. Furthermore, it synthesizes 24 kHz high-fidelity speech  $44.72 \times$  faster than real-time on a GPU.

We organize the rest of the paper as follows. We discuss related work in § 2 and present BigVGAN in § 3. We report empirical results in § 4 and conclude the paper in § 5.

## 2 Related Work

Our work builds upon the state-of-the-art of GANs for image and audio synthesis. GAN was originally proposed for image synthesis [8, 43]. Since then, impressive results have been obtained through highly optimized architectures [e.g., 17] or large scale adversarial training [e.g., 4].

Previous works on GAN-based neural vocoder focus on improving the discriminator architectures or adding new auxiliary training losses. MelGAN [22] introduces the multi-scale discriminator (MSD) that uses average pooling to downsample the raw waveform at multiple scales and applies window-based discriminators at each scale separately. It enforces the mapping between input mel spectrogram and generated waveform via an  $\ell_1$  reconstruction loss in discriminator feature space. In contrast, GAN-TTS [3] uses an ensemble of discriminators which operate on random windows of different sizes, and enforces the mapping between the conditioner and waveform adversarially using conditional discriminators. Parallel WaveGAN [56] extends the single short-time Fourier transform (STFT) loss [38] to multi-resolution, and adds it as an auxiliary loss for GAN training. Yang et al. (2021) [57] and Mustafa et al. (2022) [33] further improve MelGAN by incorporating this multi-resolution STFT loss. HiFi-GAN [19] reuses the MSD from MelGAN, while introducing the multi-period discriminator (MPD) which turns out to be a key design for high-fidelity synthesis. UnivNet [10, 11] uses the multi-resolution discriminator (MRD), which takes the multi-resolution spectrograms as the input and sharpens the spectral structure of the generated waveforms.

In this work, we focus on improving the generator by introducing a periodic inductive bias and addressing the feature aliasing issues within the non-autoregressive convolutional architecture. Our generator has a connection with the results in time-series prediction [27] and image synthesis [17].

---

<sup>4</sup>For example, WaveRNN [15] and DiffWave [20] synthesize faster than real-time with small footprint, but they are still much slower than GAN vocoder.

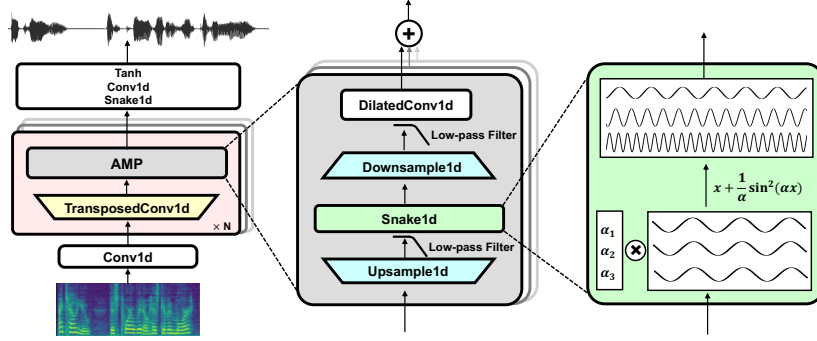


Figure 1: Schematic diagram of BigVGAN generator. The generator is composed of multiple blocks of transposed 1-D convolution followed by the proposed *anti-aliased multi-periodicity composition* (AMP) module. The AMP module adds features from multiple residual blocks with different channel-wise periodicities for different dilated 1-D convolutions. It applies *Snake* function for periodic inductive bias, and filtered nonlinearities for anti-aliasing purpose.

In contrast, CARGAN [32] incorporates the partial autoregression [40] into generator that trades synthesis speed for accurate modeling of periodicity.

There are limited investigations toward universal neural vocoding due to the noticeable challenges. In previous work, WaveRNN has been applied for universal vocoding [28, 37]. Jiao et al. (2021) [14] builds the non-autoregressive universal vocoder with Parallel WaveNet [53]. These models are capable of synthesising a wide range of speakers when the recording conditions are studio-quality, but the quality heavily degrades with varied recording conditions, non-speech vocalizations, or singing.

### 3 Method

In this section, we introduce the preliminaries for GAN vocoder, then present our BigVGAN generator. See Figure 1 for an illustration and refer to the Appendix A for a detailed architectural description. Furthermore, we identify and address the training instabilities with large-scale GAN vocoder.

#### 3.1 Preliminaries of GAN Vocoder

**Generator** The generator network takes mel spectrogram as input and output the corresponding raw waveform. In previous studies, several generator architectures have been applied, including WaveNet architecture [e.g., 56], or convolutional network that gradually upsamples the mel spectrogram to high-resolution waveform with a stack of residual blocks [e.g., 22, 19]. Note that, You et al. (2021) [58] suggests that different generator architectures can perform equally well for single-speaker neural vocoding in clean environment. In this work, we demonstrate that improving generator architecture is crucial for universal neural vocoding in challenging conditions. We choose the HiFi-GAN generator as the baseline architecture. We believe the proposed techniques are applicable to other generator architectures as well.

**Discriminator** The state-of-the-art GAN vocoders usually comprise several types of discriminators to guide the generator to synthesize coherent waveform while minimizing perceptual artifacts which are easily detectable by human ears. Importantly, each discriminator contains multiple sub-discriminators operating on different resolution windows of the waveform. For example, HiFi-GAN [19] applies two types of the discriminators: *i*) the multi-period discriminator (MPD), where the 1-D signal is reshaped to 2-D representations with varied heights and widths to separately capture the multiple periodic structures though 2-D convolutions. *ii*) The multi-scale discriminator (MSD) [22], where each sub-discriminator receives down-sampled 1-D signals at different frequency by average pooling in the time domain. A few recent works [10, 11] propose to apply the discriminator on the time-frequency domain using the multi-resolution discriminator (MRD). MRD is also composed of several sub-discriminators that operate on multiple 2-D linear spectrograms with different STFT resolutions. We also find that replacing MSD to MRD improves the quality by sharpening the signal in the spectral domain with reduced pitch and periodicity artifacts.

**Training objectives** Our training objective is similar as HiFi-GAN [19], with an exception of replacing MSD to MRD. It comprises the weighted sum of the least-square adversarial loss [29], the

feature matching loss [23], and the spectral  $\ell_1$  regression loss on mel spectrogram. We leave the details of each loss and hyper-parameters in the Appendix B.

### 3.2 Periodic Inductive Bias

The audio waveform is known to exhibit high periodicity and can be represented as a composition of primitive periodic components. This suggests that we need to provide the desired inductive bias to the generator architecture. However, the current non-autoregressive GAN vocoders [e.g., 19] solely rely on layers of dilated convolutions to learn the required periodic components at different frequencies. Their pointwise activation functions (e.g., Leaky ReLU) can only produce new details with necessary nonlinearities, but do not provide any periodic inductive bias. Furthermore, we identified that Leaky ReLU behaves poorly for *extrapolation* in waveform domain: although the model can generate high-quality speech signal in a clean (or seen) recording environment used in training, the performance degrades significantly for out-of-distribution scenarios such as unseen recording environments or instrumental audio.

We provide a proper inductive bias of periodicity to the generator by applying a recently proposed periodic activation called *Snake* function [27], defined as  $f_\alpha(x) = x + \frac{1}{\alpha} \sin^2(\alpha x)$ , where  $\alpha$  is a trainable parameter that controls the frequency of the periodic part of the signal and larger  $\alpha$  gives higher frequency. The use of  $\sin^2(x)$  ensures monotonicity and renders it amenable to easy optimization. This periodic activation exhibits an improved extrapolation capability beyond a bounded region learned by the neural network for temperature and financial data prediction [27]. In BigVGAN, we replace Leaky ReLUs with *Snake* activations  $f_\alpha(x)$  using channel-wise trainable parameters  $\alpha \in \mathbb{R}^h$  that define the periodic frequencies for each 1-D convolution channels. With this learned frequency control, the convolution kernels have more degrees of freedom to model audio waveform with multi-periodic components. In this work, we demonstrate that our *Snake*-based generator is more robust for out-of-distribution audio samples unseen during training, indicating strong extrapolation capabilities in universal vocoding.

### 3.3 Anti-aliased Representation

StyleGAN3 [17] identifies that the aliasing artifacts in image synthesis are rooted in careless signal processing. The aliasing can occur at different parts of the generator architecture, such as upsampling layers and nonlinearities in a discrete sampling grid. It introduces a variety of methods that ensure translation equivariance by interpreting the signals as continuous functions, thereby eliminating aliasing in the feature space. Instead of applying the pointwise nonlinearity in the discrete sampling grid, StyleGAN3 applies the nonlinearity to the temporarily increased resolution (e.g.  $2\times$ ) that approximates the continuous representation inspired by the Nyquist-Shannon sampling theorem [49]. The continuous representation of nonlinearity ensures translation equivariance in the feature space, and the nonlinearity generates novel frequencies in the continuous domain which is free from aliasing.

For audio synthesis, the *Snake* nonlinearity provides the required periodic inductive bias for modeling raw waveform, but applying it in the continuous feature space may also produce arbitrary high frequencies that can not be represented in the discrete-time output later. This side effect can be suppressed by applying a low-pass filter [17]. The anti-aliased nonlinearity operates by upsampling the signal by  $2\times$  along time dimension, applying the *Snake* activation, then downsampling the signal by  $2\times$ . Each upsampling and downsampling is accompanied by the low-pass filter using a windowed sinc filter with a Kaiser window [35]. Refer to the Appendix A for details.

We apply this filtered *Snake* nonlinearity in every residual dilated convolution layers within the generator to obtain the anti-aliased representation of the periodic 1-D signals. The module is named as *anti-aliased multi-periodicity composition* (AMP). See Figure 1 for an illustration. We find that incorporating the filtered activation can reduce the high-frequency artifacts in the synthesized waveform and provide significant improvements in various objective and subjective evaluations. Note that we also explored anti-aliased upsampling layers, but this results in significant training instabilities and lead to early collapse for large models. See Appendix C for more details.

### 3.4 BigVGAN with Large Scale Training

In this subsection, we set out to explore the limits of universal neural vocoding by scaling up the generator’s model capacity to its maximum while maintaining the stability of GAN training and practical usability as a high-speed neural vocoder. We start scaling up the model with our improved

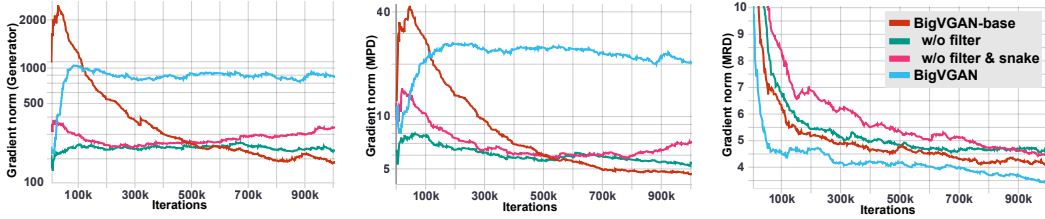


Figure 2: Visualization of gradient norm for different modules from BigVGAN training. Left: Gradient norm from the generator. Mid: Gradient from the MPD module. Right: Gradient norm from the MRD module. For BigVGAN-base, the gradient norm significantly increases at early training without clipping. For BigVGAN, the gradient will explode without clipping.

generator using the comparable V1 configuration of HiFi-GAN [19] with 14M parameters, which is denoted as BigVGAN-base. We grow BigVGAN-base by increasing the number of upsampling blocks and convolution channels for each block. The BigVGAN-base upsamples the signal by  $256\times$  using 4 upsampling blocks with the ratio of [8, 8, 2, 2]. Each upsampling block is accompanied by multiple residual layers with dilated convolutions, i.e., the AMP module. We further divide the  $256\times$  upsampling into 6 blocks [4, 4, 2, 2, 2, 2] for more fine-grained feature refinement. In addition, we increase the number of channels of AMP module (analogous to MRF in HiFi-GAN) from 512 to 1536. We denote the model with 1536 channels and 112M parameters as BigVGAN.

We found that the default learning rate of  $2 \times 10^{-4}$  used in HiFi-GAN causes an early training collapse for BigVGAN training, where the losses from the discriminator submodules immediately converge to zero after several thousands of iterations. Halving the learning rate to  $1 \times 10^{-4}$  was able to reduce such failures. We also found that large batch size is helpful to reduce mode collapse, as it covers more modes per batch. We simply double the batch size from the usual 16 to 32 for a good trade-off between training efficiency and stability, as neural vocoders can require millions of steps to converge. Our required batch size is much smaller than the observed one for large scale GAN training in image domain (i.e., 32 vs. 2048) [4], probably thanks to the strong conditioner in neural vocoding.

We observed that large BigVGAN can still be prone to collapse early in training, even with the aforementioned changes. We track the gradient norm of each module during training and identify that the anti-aliased nonlinearity significantly amplified the gradient norm of MPD. Consequently, BigVGAN generator receives a diverging gradient early in training, leading to instabilities and potential collapse. We visualize the norm of gradient for each module in Figure 2. We alleviate the issue by clipping the global norm of the gradient to  $10^3$ , which is close to the average gradient norm of the 112M BigVGAN generator. This gradient clipping prevents the early training collapse by regularizing the early divergence of the generator. Note that, gradient clipping was found ineffective to alleviate training instability for large scale GAN on images (see Appendix H in [4]), but it is very effective in our audio endeavors.

In addition to above efforts, we have explored other directions, including various ways to improve the model architecture, spectral normalization [31] to stabilize GAN training, and data augmentation to improve model generalization. Unfortunately, all these trials resulted in worse perceptual quality in our study. The details can be found in the Appendix C. We hope these practical lessons that we have learned would be useful to future research endeavors.

## 4 Results

In this section, we present a comprehensive study of BigVGAN to evaluate the zero-shot vocoding performance in diverse scenarios, such as unseen recording environments, unseen speakers and languages, and out-of-distribution data including singing voice and instrumental audio.

### 4.1 Training Data

We use LibriTTS [60] dataset with the original sampling rate of 24,000Hz for training. Unlike previous studies which only adopted a subset (train-clean-100 or train-clean-360) recorded in a clean environment [10, 11, 1], we use all training data including the subset from diverse and noisy recording environments (LibriTTS-full = train-clean-100 + train-clean-360 + train-other-500), which is unprecedented in the literature. We find that the diversity of the

Table 1: Model footprint and synthesis speed measured on an NVIDIA RTX 8000 GPU.

Method	HiFi-GAN (V1)	BigVGAN-base	w/o filter	BigVGAN
Params (M)	14.01	14.01	14.01	112.4
Syn. speed	93.75 ×	70.18 ×	75.83 ×	44.72 ×

training data is important to achieve the goal towards universal neural vocoding using BigVGAN.<sup>5</sup> For our zero-shot experiments on unseen dataset, we resample the audio to 24,000Hz if necessary using `kaiser-best` algorithm provided by `librosa` Python package.

Conventional STFT parameters are engineered to have a limited frequency band [0, 8,000] Hz by cutting off the high frequency details for easier modeling. On a contrary, we train all models (including the baselines) using a full-band frequency [0, 12,000] Hz and a 100-band log-mel spectrogram, which is also used in a recent study towards universal vocoding [11]. We set other STFT parameters as in previous work [19], with 1024 FFT size, 1024 Hann window, and 256 hop size.

## 4.2 Models

We train all BigVGAN models including the ablation models and the baseline HiFi-GAN using our training configuration for 1M steps. We use the batch size of 32, a segment size of 8,192, and a initial learning rate of  $1 \times 10^{-4}$ . All other configurations including optimizer, learning rate scheduler, and scalar weights of the loss terms follow the official open-source implementation of HiFi-GAN [19] without modification, with an exception that BigVGAN replaces MSD by MRD for the discriminator. All models are trained using NVIDIA DGX-1 with 8 V100 GPUs. Refer to Table 7 in the Appendix A for detailed hyperparameters. For out-of-distribution test, we also include the unofficial open-source implementation<sup>6</sup> of pretrained UnivNet-c32 [11] which is reported to outperform HiFi-GAN for the same training configurations and used `train-clean-360` subset for training. We also include a comparison with SC-WaveRNN [37], a universal neural vocoder based on WaveRNN, using its official implementation. See appendix D for more details.

Table 1 summarizes the model footprint and synthesis speed of GAN vocoders for generating 24,000Hz audio. BigVGAN-base with 14M parameters can synthesize the audio 70.18 × faster than real time. BigVGAN features fast inference speed due to fully non-autoregressive architecture, but it is slower than HiFi-GAN as the filtered *Snake* function requires more computation. Our largest BigVGAN with 112M parameters can synthesize the audio 44.72 × faster than real-time and keeps the promise as a high-speed neural vocoder.

## 4.3 Evaluation Metrics

The objective metrics we collected are designed to measure varied types of distance between the ground-truth audio and the generated sample. We provide 5 different metrics: 1) Multi-resolution STFT (M-STFT) [56] which measures the spectral distance across multiple resolutions.<sup>7</sup> 2) Perceptual evaluation of speech quality (PESQ) [47], a widely adopted automated assessment of voice quality.<sup>8</sup> 3) Mel-cepstral distortion (MCD) [21] with dynamic time warping which measures the difference between mel cepstra.<sup>9</sup> 4) Periodicity error, and 5) F1 score of voiced/unvoiced classification (V/UV F1) which are considered as major artifacts from non-autoregressive GAN vocoders [32].<sup>10</sup>

The subjective evaluation of universal neural vocoder is challenging, in that the model needs to encompass diverse speaker identities and recording environments. In an extreme case, the model may always output some very natural “average” voices, which is not preferred but can still be highly rated by human workers in conventional 5-scale mean opinion score (MOS) evaluation. Furthermore, the state-of-the art GAN vocoders [19] are reaching to near parity with the ground-truth naturalness under studio-quality recording condition, thus the gap of subjective scores between models under clean condition has been narrowed.

<sup>5</sup>The ablation results on training data diversity can be found in Table 6.

<sup>6</sup><https://github.com/mindslab-ai/univnet>. Note there is no official open-source implementation.

<sup>7</sup>We used an open-source implementation from Auraloss [51].

<sup>8</sup>We used a 16,000Hz wide-band implementation from <https://github.com/ludlows/python-pesq>.

<sup>9</sup>We used an open-source implementation from <https://github.com/ttslr/python-MCD>.

<sup>10</sup>We used the periodicity error and V/UV F1 score implementation provided by CARGAN [32].

Table 2: Objective and subjective quality metrics of BigVGAN evaluated on **clean** subsets of LibriTTS. Objective results are obtained from `dev-clean`, and subjective evaluations with 5-scale mean opinion score (MOS) and similarity mean opinion score (SMOS) with 95% confidence interval (CI) are obtained from `test-clean`.

LibriTTS (clean)	M-STFT(↓)	PESQ(↑)	MCD(↓)	Periodicity(↓)	V/UV F1(↑)	MOS(↑)	SMOS(↑)
Ground Truth	-	-	-	-	-	4.51±0.05	4.63±0.05
HiFi-GAN (V1)	0.9773	3.042	0.6257	0.1545	0.9306	4.21±0.08	4.49±0.07
BigVGAN-base	0.8675	3.569	0.4429	0.1295	0.9453	4.18±0.07	4.49±0.07
BigVGAN	<b>0.8151</b>	<b>3.896</b>	<b>0.3591</b>	<b>0.1106</b>	<b>0.9564</b>	<b>4.29±0.07</b>	<b>4.54±0.06</b>

Table 3: Objective and subjective quality metrics of BigVGAN evaluated on **other** subsets of LibriTTS. Objective results are obtained from `dev-other` and subjective evaluations with 5-scale MOS and SMOS with 95% CI are obtained from `test-other`.

LibriTTS (other)	M-STFT(↓)	PESQ(↑)	MCD(↓)	Periodicity(↓)	V/UV F1(↑)	MOS(↑)	SMOS(↑)
Ground Truth	-	-	-	-	-	4.35±0.05	4.62±0.05
HiFi-GAN (V1)	1.026	2.853	0.6948	0.1585	0.9294	4.15±0.08	4.47±0.07
BigVGAN-base	0.9052	3.502	0.4776	0.1357	0.9403	4.18±0.07	4.54±0.07
BigVGAN	<b>0.8517</b>	<b>3.825</b>	<b>0.3906</b>	<b>0.1218</b>	<b>0.9486</b>	<b>4.26±0.07</b>	<b>4.56±0.07</b>

In addition to the conventional 5-scale mean opinion score (MOS) of audio naturalness, we also take the 5-scale similarity mean opinion score (SMOS) as the major evaluation metric where the participant is directly asked to give the score of similarity for the pair of audio after listening to ground-truth audio and the sample from the model side-by-side. SMOS provides an improved way assessing how close the given sample is to the ground-truth, where the ground-truth recordings can have diverse speaker identities, contain unseen languages and be recorded in diverse environments. It is also directly applicable to non-speech samples. We used Mechanical Turk to perform MOS and SMOS tests with 450 unique ratings per model. To encompass diverse participants, we allowed the participant to evaluate only up to three randomly exposed samples.

#### 4.4 LibriTTS Results

We report the performance of BigVGAN and the baseline models evaluated on LibriTTS using the previously mentioned objective and subjective metrics. We conduct the experiments with two types of subsets: one is from clean recording environments with unseen speakers (`dev-clean`, `test-clean`), and the other is from diverse and noisy recording environments with unseen speakers (`dev-other`, `test-other`). We perform objective evaluations using development sets, and conduct subjective evaluations using the randomly selected 100 audio clips from test sets.

Table 2 shows the experimental results from the LibriTTS `clean` evaluation sets. BigVGAN significantly improves all objective metrics. In particular, BigVGAN-base with 14M parameters same as HiFi-GAN (V1) exhibits consistently improved objective scores, suggesting that it has better periodic inductive bias for waveform data. Both BigVGAN-base and HiFi-GAN (V1) with 14M parameters perform comparably well in terms of MOS ( $\pm 0.03$ ) and SMOS ( $\pm 0.00$ ) evaluations. This suggests that for the model with restricted capacity, the clean speech evaluation set is not challenging enough to differentiate the state-of-the-art GAN vocoder architectures under human listening test. In contrast, 112M BigVGAN can measurably outperform HiFi-GAN in terms of MOS ( $\pm 0.08$ ) and SMOS ( $\pm 0.05$ ) evaluation, because it has high model capacity to further leverage the diverse training data for better quality.

Table 3 shows the same suite of results on the LibriTTS `other` evaluation sets. Similar as the results on clean subsets, BigVGAN-base shows consistent improvements for all objective metrics due to the periodic inductive bias. BigVGAN-base performs comparably well as HiFi-GAN in terms of MOS ( $\pm 0.03$ ) and measurably better in terms of SMOS ( $\pm 0.07$ ). It suggests that BigVGAN-base’s extrapolation capability is still unsung for subjective evaluation under similar recording environments that have been seen at training [60]. However, the 112M BigVGAN consistently outperforms HiFi-GAN by a clear margin for both MOS ( $\pm 0.11$ ) and SMOS ( $\pm 0.09$ ). This further indicates that BigVGAN can leverage the large LibriTTS speech corpus and continue to improve its synthesis quality up to the unprecedented model size without saturation.

Table 4: The 5-scale SMOS results evaluated on unseen languages with different types of noise in unseen recording environments. †: pretrained weight obtained from an open-source repository which used `train-clean-360` subset for training.

Recording env. Language	Clean Jv,Km,Ne,Su	Noisy (sim) Es,Fr,It,Pt	Noisy (real) Ko
Ground Truth	4.58±0.05	4.36±0.05	4.56±0.05
UnivNet-c32†	4.35±0.07	3.95±0.09	4.18±0.08
HiFi-GAN (V1)	4.39±0.07	4.13±0.08	4.21±0.08
BigVGAN-base	4.38±0.07	4.21±0.07	4.36±0.07
BigVGAN	<b>4.41±0.07</b>	<b>4.26±0.07</b>	<b>4.38±0.07</b>

Table 5: The 5-scale SMOS results evaluated on out-of-distribution samples with MUSDB18-HQ. †: pretrained weight obtained from an open-source repository which used `train-clean-360` subset for training.

Method	Vocal	Drums	Bass	Others	Mixture	Average
Ground Truth	4.58±0.05	4.57±0.05	4.52±0.05	4.61±0.05	4.56±0.05	4.57±0.02
UnivNet-c32†	4.22±0.09	4.23±0.09	3.90±0.11	3.80±0.13	3.80±0.12	3.99±0.05
HiFi-GAN (V1)	4.26±0.08	4.37±0.08	3.95±0.11	3.92±0.12	3.91±0.11	4.08±0.05
BigVGAN-base	4.36±0.08	4.39±0.07	<b>4.00 ±0.11</b>	4.14±0.09	4.11±0.10	4.20±0.04
w/o filter	4.30±0.08	4.32±0.07	3.95±0.11	4.05±0.10	4.11±0.10	4.15±0.04
w/o filter & snake	4.31±0.08	4.32±0.07	3.94±0.11	4.01±0.11	4.02±0.10	4.12±0.04
BigVGAN	<b>4.37±0.08</b>	<b>4.41±0.07</b>	<b>4.00±0.10</b>	<b>4.25±0.09</b>	<b>4.26±0.08</b>	<b>4.26±0.04</b>

In Appendix D, we also report the expanded evaluation results, including ablation models, SC-WaveRNN [37], and UnivNet [11] on LibriTTS, unseen VCTK [55], and LJSpeech [9] data.

#### 4.5 Unseen Languages and Recording Environments

In this subsection, we assess the universal vocoding capability of BigVGAN by measuring its zero-shot performance for various unseen languages with varied types of the recording environments in the unseen dataset. We gather three classes of a publicly available multi-language dataset categorized by the type of noise from the recording environment.

- A collection of under-resourced languages recorded in a noiseless studio environment [50]: Javanese, Khmer, Nepali, and Sundanese. We use randomly selected 50 audio clips with equal balance across languages from the combined dataset.
- The Multilingual TEDx Corpus [48]: contains a collection of TEDx talks in Spanish, French, Italian, and Portuguese. We use randomly selected 50 audio clips with equal balance across languages from the IWSLT’21 test set. We simulate the unseen recording environment setup by adding a random environmental noise from MS-SNSD [46], such as airport, cafe, babble, etc.
- Deeply Korean read speech corpus [7]: contains short speech audio clips in Korean, recorded in three types of recording environments (anechoic chamber, studio apartment, and dance studio) using a smartphone. We use randomly selected 50 audio clips where 25 clips are from the studio apartment, and the remaining 25 clips are from the dance studio. The collected audio clips contain a significant amount of noise and artifacts from real-world recording environments, such as reverb, echo, and static background noise.

Table 4 summarizes the SMOS results from three different types of unseen dataset. We only did SMOS evaluations, because the datasets have unseen languages for human listeners and it is hard to determine the quality without side-by-side comparison with ground-truth. For clean under-resourced language dataset, the performance gap between models is not substantially large similar to the clean speech results from Section 4.4. This indicates that the universal vocoder trained on the entire LibriTTS training sets is robust to unseen languages under clean recording environments. For both types of unseen recording environment (simulated or real-world), BigVGAN outperforms the baseline models by a large margin. The small capacity BigVGAN-base also shows improvements compared to the baseline with statistical significance (p-value < 0.05 from the Wilcoxon signed-rank test). This suggests that BigVGAN is significantly more robust to the unseen recording environments thanks to the improved generator design with the AMP module.



Table 6: Ablation results on training data diversity using 112M BigVGAN model, evaluated on LibriTTS. Objective results are obtained from `dev-other` and subjective evaluation with 5-scale SMOS with 95% confidence interval (CI) is obtained from `test-other`.

Training data	M-STFT(↓)	PESQ(↑)	MCD(↓)	Periodicity(↓)	V/UV F1(↑)	SMOS(↑)
Ground Truth	-	-	-	-	-	4.55±0.05
LibriTTS- <code>full</code>	<b>0.8517</b>	<b>3.825</b>	<b>0.3906</b>	<b>0.1218</b>	<b>0.9486</b>	<b>4.38±0.07</b>
<code>train-clean-360</code>	0.8882	3.597	0.4680	0.1405	0.9389	4.31±0.08
VCTK	0.9247	3.586	0.6715	0.1405	0.9395	4.27±0.08

We also test the open-source implementation of UnivNet [11] with the pretrained checkpoint which is trained on `train-clean-360` subset. Contrary to the report from [11] that UnivNet-c32 outperformed HiFi-GAN [19], we find that the unmodified HiFi-GAN trained on the entire LibriTTS dataset is able to match or outperform UnivNet-c32. We also train UnivNet-c32 on LibriTTS-`full` and find that it is not benefited from larger training data. See Appendix D for detailed analysis.

#### 4.6 Out-of-Distribution Robustness

In this subsection, we test BigVGAN’s robustness and extrapolation capability by measuring zero-shot performance on out-of-distribution data. We conduct the SMOS experiment using MUSDB18-HQ [44], a multi-track music audio dataset which contains vocal, drums, bass, other instruments, and the original mixture. The test set contains 50 songs with 5 tracks. We gather the mid-song clip with the duration of 10 seconds for each track and song.

Table 5 shows the SMOS results from the 5 tracks and their average from the MUSDB18-HQ test set. BigVGAN models demonstrate a substantially improved zero-shot generation performance with wider frequency band coverage, whereas baseline models fail to generate audio outside the limited frequency range and suffer from severe distortion. The improvements are most profound for singing voice (vocal), instrumental audio (others) and the full mixture of the song (mixture), whereas the improvements from drums and bass are less significant. UnivNet-c32 trained on `train-clean-360` still vastly underperforms the unmodified HiFi-GAN trained on full LibriTTS data.

We also experiment with audios obtained from YouTube videos from real-world recording environments. BigVGAN also exhibits robustness to various types of out-of-distribution signals such as laughter. We provide audio samples to our demo page.<sup>11</sup>

#### 4.7 Ablation Study

**Model architecture** To measure the effectiveness of the BigVGAN generator, we include SMOS test for the ablation models of BigVGAN-base on MUSDB18-HQ data. Table 5 shows that the ablation models exhibit clear degradation on various scenarios such as instrumental audio (others, mixture). From the average SMOS ratings, disabling the filter for *Snake* activation performs worse than BigVGAN-base and removing both the filter and *Snake* activation is even worse than the *Snake*-only ablation model, both with statistical significance (p-value < 0.01 from the Wilcoxon signed-rank test). This indicates that Leaky ReLU is not robust enough to extrapolate beyond the learned frequency range and the aliasing artifacts degrade the audio quality in challenging setups. The results show that BigVGAN generator demonstrates strong robustness and extrapolation capability to out-of-distribution scenarios because of the seamless integration of periodic inductive bias and anti-aliased feature representation.

**Data diversity** To verify the importance of the scale and diversity of the training data, we trained our BigVGAN using less diverse, clean speech-only dataset with the same training configuration for 1M steps: 1) `train-clean-360` subset of LibriTTS, or 2) VCTK dataset. Table 6 shows that training BigVGAN on less diverse data shows degradation in both objective metrics and the subjective SMOS on the LibriTTS evaluation sets. The result verifies the importance of using diverse training data and demonstrates the effectiveness of BigVGAN on large-scale datasets.

<sup>11</sup><https://bigvgan-demo.github.io>

## 5 Conclusions

This study explores the limits of universal neural vocoding with an unprecedented scale and analyzes the performance across diverse scenarios including unseen speakers, languages, recording environments and out-of-distribution data. We present BigVGAN with an improved generator architecture by introducing anti-aliased periodic activation function with learned frequency control, which injects the desired inductive bias for waveform synthesis. Armed with the improved generator, we demonstrate the largest non-autoregressive GAN vocoder with strong zero-shot performance under various conditions, including unseen recording environments, singing voice, and instrumental audio. We believe that BigVGAN, combined with practical lessons learned from the large scale training, will inspire future endeavors for universal neural vocoding and improve the state-of-the-art results for real-world applications, such as voice cloning, voice conversion, speech translation, and audio codec.

## References

- [1] E. A. AlBadawy, A. Gibiansky, Q. He, J. Wu, M.-C. Chang, and S. Lyu. Vocbench: A neural vocoder benchmark for speech synthesis. In *ICASSP*, 2022.
- [2] S. O. Arik, J. Chen, K. Peng, W. Ping, and Y. Zhou. Neural voice cloning with a few samples. In *NeurIPS*, 2018.
- [3] M. Bińkowski, J. Donahue, S. Dieleman, A. Clark, E. Elsen, N. Casagrande, L. C. Cobo, and K. Simonyan. High fidelity speech synthesis with adversarial networks. In *ICLR*, 2020.
- [4] A. Brock, J. Donahue, and K. Simonyan. Large scale gan training for high fidelity natural image synthesis. In *ICLR*, 2019.
- [5] T. B. Brown, B. Mann, N. Ryder, M. Subbiah, J. Kaplan, P. Dhariwal, A. Neelakantan, P. Shyam, G. Sastry, A. Askell, et al. Language models are few-shot learners. In *NeurIPS*, 2020.
- [6] N. Chen, Y. Zhang, H. Zen, R. J. Weiss, M. Norouzi, and W. Chan. WaveGrad: Estimating gradients for waveform generation. In *ICLR*, 2021.
- [7] Deeply. Deeply Korean read speech corpus, 2021.
- [8] I. Goodfellow, J. Pouget-Abadie, M. Mirza, B. Xu, D. Warde-Farley, S. Ozair, A. Courville, and Y. Bengio. Generative adversarial nets. In *NeurIPS*, 2014.
- [9] K. Ito. The LJ speech dataset. 2017.
- [10] W. Jang, D. Lim, and J. Yoon. Universal melgan: A robust neural vocoder for high-fidelity waveform generation in multiple domains. In *arXiv preprint arXiv:2011.09631*, 2020.
- [11] W. Jang, D. Lim, J. Yoon, B. Kim, and J. Kim. UnivNet: A neural vocoder with multi-resolution spectrogram discriminators for high-fidelity waveform generation. In *Interspeech*, 2021.
- [12] Y. Jia, R. J. Weiss, F. Biadsy, W. Macherey, M. Johnson, Z. Chen, and Y. Wu. Direct speech-to-speech translation with a sequence-to-sequence model. In *Interspeech*, 2019.
- [13] Y. Jia, Y. Zhang, R. J. Weiss, Q. Wang, J. Shen, F. Ren, Z. Chen, P. Nguyen, R. Pang, I. L. Moreno, et al. Transfer learning from speaker verification to multispeaker text-to-speech synthesis. In *NeurIPS*, 2018.
- [14] Y. Jiao, A. Gabryś, G. Tinchev, B. Putrycz, D. Korzekwa, and V. Klimkov. Universal neural vocoding with parallel wavenet. In *ICASSP*, 2021.
- [15] N. Kalchbrenner, E. Elsen, K. Simonyan, S. Noury, N. Casagrande, E. Lockhart, F. Stimberg, A. v. d. Oord, S. Dieleman, and K. Kavukcuoglu. Efficient neural audio synthesis. In *ICML*, 2018.
- [16] T. Karras, M. Aittala, J. Hellsten, S. Laine, J. Lehtinen, and T. Aila. Training generative adversarial networks with limited data. In *NeurIPS*, 2020.
- [17] T. Karras, M. Aittala, S. Laine, E. Härkönen, J. Hellsten, J. Lehtinen, and T. Aila. Alias-free generative adversarial networks. In *NeurIPS*, 2021.
- [18] S. Kim, S.-g. Lee, J. Song, and S. Yoon. FloWaveNet: A generative flow for raw audio. In *ICML*, 2019.
- [19] J. Kong, J. Kim, and J. Bae. HiFi-GAN: Generative adversarial networks for efficient and high fidelity speech synthesis. In *NeurIPS*, 2020.

- [20] Z. Kong, W. Ping, J. Huang, K. Zhao, and B. Catanzaro. DiffWave: A versatile diffusion model for audio synthesis. In *ICLR*, 2021.
- [21] R. Kubichek. Mel-cepstral distance measure for objective speech quality assessment. In *Proceedings of IEEE Pacific Rim Conference on Communications Computers and Signal Processing*, volume 1, pages 125–128. IEEE, 1993.
- [22] K. Kumar, R. Kumar, T. de Boissiere, L. Gestin, W. Z. Teoh, J. Sotelo, A. de Brébisson, Y. Bengio, and A. C. Courville. MelGan: Generative adversarial networks for conditional waveform synthesis. In *NeurIPS*, 2019.
- [23] A. B. L. Larsen, S. K. Sønderby, H. Larochelle, and O. Winther. Autoencoding beyond pixels using a learned similarity metric. In *ICML*, 2016.
- [24] S.-g. Lee, H. Kim, C. Shin, X. Tan, C. Liu, Q. Meng, T. Qin, W. Chen, S. Yoon, and T.-Y. Liu. Priorgrad: Improving conditional denoising diffusion models with data-dependent adaptive prior. In *ICLR*, 2022.
- [25] S.-g. Lee, S. Kim, and S. Yoon. Nanoflow: Scalable normalizing flows with sublinear parameter complexity. In *NeurIPS*, 2020.
- [26] L.-J. Liu, Z.-H. Ling, Y. Jiang, M. Zhou, and L.-R. Dai. Wavenet vocoder with limited training data for voice conversion. In *Interspeech*, 2018.
- [27] Z. Liu, T. Hartwig, and M. Ueda. Neural networks fail to learn periodic functions and how to fix it. In *NeurIPS*, 2020.
- [28] J. Lorenzo-Trueba, T. Drugman, J. Latorre, T. Merritt, B. Putrycz, R. Barra-Chicote, A. Moinet, and V. Aggarwal. Towards achieving robust universal neural vocoding. In *Interspeech*, 2019.
- [29] X. Mao, Q. Li, H. Xie, R. Y. Lau, Z. Wang, and S. Paul Smolley. Least squares generative adversarial networks. In *ICCV*, 2017.
- [30] S. Mehri, K. Kumar, I. Gulrajani, R. Kumar, S. Jain, J. Sotelo, A. Courville, and Y. Bengio. SampleRNN: An unconditional end-to-end neural audio generation model. In *ICLR*, 2017.
- [31] T. Miyato, T. Kataoka, M. Koyama, and Y. Yoshida. Spectral normalization for generative adversarial networks. In *ICML*, 2018.
- [32] M. Morrison, R. Kumar, K. Kumar, P. Seetharaman, A. Courville, and Y. Bengio. Chunked autoregressive gan for conditional waveform synthesis. In *ICLR*, 2022.
- [33] A. Mustafa, N. Pia, and G. Fuchs. Stylemelgan: An efficient high-fidelity adversarial vocoder with temporal adaptive normalization. In *ICASSP*, 2021.
- [34] A. Odena, V. Dumoulin, and C. Olah. Deconvolution and checkerboard artifacts. *Distill*, 2016.
- [35] A. V. Oppenheim and R. W. Schaffer. *Discrete-Time Signal Processing*. 2009.
- [36] D. S. Park, W. Chan, Y. Zhang, C.-C. Chiu, B. Zoph, E. D. Cubuk, and Q. V. Le. Specaugment: A simple data augmentation method for automatic speech recognition. In *Interspeech*, 2019.
- [37] D. Paul, Y. Pantazis, and Y. Stylianou. Speaker conditional WaveRNN: Towards universal neural vocoder for unseen speaker and recording conditions. In *Interspeech*, 2020.
- [38] W. Ping, K. Peng, and J. Chen. ClariNet: Parallel wave generation in end-to-end text-to-speech. In *ICLR*, 2019.
- [39] W. Ping, K. Peng, A. Gibiansky, S. O. Arik, A. Kannan, S. Narang, J. Raiman, and J. Miller. Deep Voice 3: Scaling text-to-speech with convolutional sequence learning. In *ICLR*, 2018.
- [40] W. Ping, K. Peng, K. Zhao, and Z. Song. WaveFlow: A compact flow-based model for raw audio. In *ICML*, 2020.
- [41] J. Pons, S. Pascual, G. Cengarle, and J. Serrà. Upsampling artifacts in neural audio synthesis. In *ICASSP*, 2021.
- [42] R. Prenger, R. Valle, and B. Catanzaro. WaveGlow: A flow-based generative network for speech synthesis. In *ICASSP*, 2019.

- [43] A. Radford, L. Metz, and S. Chintala. Unsupervised representation learning with deep convolutional generative adversarial networks. In *ICLR*, 2016.
- [44] Z. Rafii, A. Liutkus, F.-R. Stöter, S. I. Mimitakis, and R. Bittner. Musdb18-hq - an uncompressed version of musdb18, Aug. 2019.
- [45] A. Ramesh, M. Pavlov, G. Goh, S. Gray, C. Voss, A. Radford, M. Chen, and I. Sutskever. Zero-shot text-to-image generation. In *ICML*, 2021.
- [46] C. K. Reddy, E. Beyrami, J. Pool, R. Cutler, S. Srinivasan, and J. Gehrke. A scalable noisy speech dataset and online subjective test framework. In *Interspeech*, 2019.
- [47] A. W. Rix, J. G. Beerends, M. P. Hollier, and A. P. Hekstra. Perceptual evaluation of speech quality (pesq)-a new method for speech quality assessment of telephone networks and codecs. In *2001 IEEE international conference on acoustics, speech, and signal processing. Proceedings (Cat. No. 01CH37221)*, volume 2, pages 749–752. IEEE, 2001.
- [48] E. Salesky, M. Wiesner, J. Bremerman, R. Cattoni, M. Negri, M. Turchi, D. W. Oard, and M. Post. The multilingual tedx corpus for speech recognition and translation. *arXiv preprint arXiv:2102.01757*, 2021.
- [49] C. E. Shannon. Communication in the presence of noise. *Proceedings of the IRE*, 1949.
- [50] K. Sodimana, K. Pipatsrisawat, L. Ha, M. Jansche, O. Kjartansson, P. De Silva, and S. Sarin. A step-by-step process for building tts voices using open source data and framework for bangla, javanese, khmer, nepali, sinhala, and sundanese. 2018.
- [51] C. J. Steinmetz and J. D. Reiss. auraloss: Audio focused loss functions in pytorch. In *Digital Music Research Network One-day Workshop (DMRN+ 15)*, 2020.
- [52] A. van den Oord, S. Dieleman, H. Zen, K. Simonyan, O. Vinyals, A. Graves, N. Kalchbrenner, A. Senior, and K. Kavukcuoglu. WaveNet: A generative model for raw audio. *arXiv preprint arXiv:1609.03499*, 2016.
- [53] A. van den Oord, Y. Li, I. Babuschkin, K. Simonyan, O. Vinyals, K. Kavukcuoglu, G. v. d. Driessche, E. Lockhart, L. C. Cobo, F. Stimberg, et al. Parallel WaveNet: Fast high-fidelity speech synthesis. In *ICML*, 2018.
- [54] A. Vaswani, N. Shazeer, N. Parmar, J. Uszkoreit, L. Jones, A. N. Gomez, Ł. Kaiser, and I. Polosukhin. Attention is all you need. In *Advances in neural information processing systems*, pages 5998–6008, 2017.
- [55] J. Yamagishi, C. Veaux, K. MacDonald, et al. Cstr vctk corpus: English multi-speaker corpus for cstr voice cloning toolkit (version 0.92). 2019.
- [56] R. Yamamoto, E. Song, and J.-M. Kim. Parallel WaveGAN: A fast waveform generation model based on generative adversarial networks with multi-resolution spectrogram. In *ICASSP*, 2020.
- [57] G. Yang, S. Yang, K. Liu, P. Fang, W. Chen, and L. Xie. Multi-band melgan: Faster waveform generation for high-quality text-to-speech. In *IEEE Spoken Language Technology Workshop*, 2021.
- [58] J. You, D. Kim, G. Nam, G. Hwang, and G. Chae. GAN vocoder: Multi-resolution discriminator is all you need. In *Interspeech*, 2021.
- [59] N. Zeghidour, A. Luebs, A. Omran, J. Skoglund, and M. Tagliasacchi. Soundstream: An end-to-end neural audio codec. *IEEE/ACM Transactions on Audio, Speech, and Language Processing*, 2021.
- [60] H. Zen, V. Dang, R. Clark, Y. Zhang, R. J. Weiss, Y. Jia, Z. Chen, and Y. Wu. Libritts: A corpus derived from librispeech for text-to-speech. In *Interspeech*, 2019.
- [61] H. Zhang, M. Cisse, Y. N. Dauphin, and D. Lopez-Paz. mixup: Beyond empirical risk minimization. In *ICLR*, 2018.

# Appendix

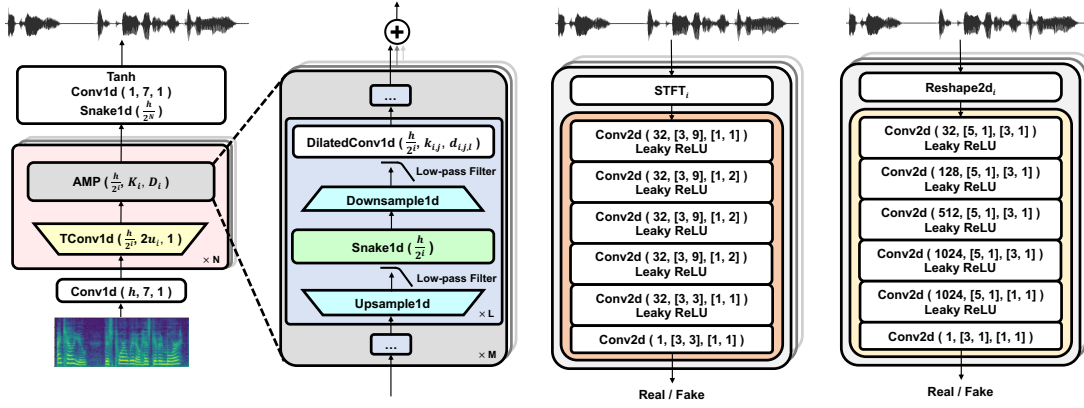


Figure 3: Detailed diagram of BigVGAN generator and discriminator architectures. Left: generator architecture, where values in parentheses denote (output channel, kernel width, dilation rate) respectively. Right: discriminator architectures (MRD in orange and MPD in yellow), where values in parentheses denote (output channel, [kernel width, kernel height], [stride width, stride height]) respectively.

Table 7: Hyperparameters of BigVGAN generators and discriminators.

	Generator		Discriminator	
	BigVGAN-base	BigVGAN	MRD & MPD	
$h$	512	1536	$n\_fft_i$	[1024, 2048, 512]
$u_i$	[8, 8, 2, 2]	[4, 4, 2, 2, 2, 2]	$hop\_length_i$	[120, 240, 50]
$K_i$	[3, 3, 3, 7, 7, 7, 11, 11, 11]	[3, 3, 3, 7, 7, 7, 11, 11, 11]	$win\_length_i$	[600, 1200, 240]
$D_i$	[[1, 1], [3, 1], [5, 1]] $\times$ 3	[[1, 1], [3, 1], [5, 1]] $\times$ 3	$Reshape2d_i(p_i)$	[2, 3, 5, 7, 11]

## A Architectural Details

In this section, we present a detailed description of the BigVGAN architecture. Refer to Figure 3 for illustrative details. BigVGAN uses the similar generator architecture presented in HiFi-GAN [19]. The generator takes a mel spectrogram as input and synthesizes a corresponding waveform as output. The generation process starts with a single layer of 1D convolution using a channel width of  $h$  and a kernel size of 7 without dilation (denoted as 1 in the Figure 3). The hierarchical generation comprises  $N$  number of upsampling blocks. The  $i$ -th upsampling block ( $i = \{1, \dots, N\}$ ) starts with a transposed 1D convolution using half the number of channels of the preceding block and an upsampling rate of  $u_i$ . The upsampled feature is followed by  $M$  number of AMP residual blocks, where each AMP block uses different kernel sizes for a stack of dilated 1D convolutions defined as  $k_{i,j}$  ( $j = \{1, \dots, M\}$ ). The  $j$ -th AMP block contains  $L$  number of the anti-aliased periodic activation and the dilated 1D convolution using a dilatation rate of  $d_{i,j,l}$  ( $l = \{1, \dots, L\}$ ). Refer to the Table 7 for the hyperparameters of the BigVGAN generators.

Our design of the low-pass filter is similar to StyleGAN3 [17]. We use a cutoff frequency of  $\frac{s}{2^m}$ , where  $m = 2$  is a up- and down-sampling ratio and  $s$  is a sampling rate (e.g., width) of the signal. The Kaiser window uses a window length of  $n = 6 \cdot m$  and a shape parameter  $\beta$  is approximated by  $0.1102 \cdot (A - 8.7)$ , where a maximum attenuation  $A$  is approximated by  $A = 2.285 \cdot (\frac{n}{2} - 1) \cdot \pi \cdot 4f_h + 7.95$  [35] with a transition band half-width  $f_h = \frac{0.6}{m}$ .

The BigVGAN discriminator comprises two submodules: MRD and MPD. Each module is composed of multiple subdiscriminators using a stack of 2D convolutions as in Figure 3. MRD converts the input 1D waveform to its 2D linear spectrogram using STFT with different parameters ( $n\_fft$ ,  $hop\_length$ ,  $win\_length$ ). MPD converts the input 1D waveform with length  $T$  to its 2D

representation by reshaping and reflection padding (Reshape2d) with different width ( $p_i$ ) and height ( $\frac{T}{p_i}$ ). Refer to the Table 7 for the MRD and MPD hyperparameters. We used the same MRD and MPD hyperparameters for training all BigVGAN generators.

## B Training Objective Details

We apply the training objective formulation and its hyperparameters described in [19] without modification, with an exception that BigVGAN applies MRD replacing MSD as the discriminator submodule. Concretely, we apply the following objectives  $\mathcal{L}_G$  for generator and  $\mathcal{L}_D$  for discriminator, respectively:

$$\mathcal{L}_G = \sum_{k=1}^K \left[ \mathcal{L}_{adv}(G; D_k) + \lambda_{fm} \mathcal{L}_{fm}(G; D_k) \right] + \lambda_{mel} \mathcal{L}_{mel}(G), \quad \mathcal{L}_D = \sum_{k=1}^K \left[ \mathcal{L}_{adv}(D_k; G) \right], \quad (1)$$

where  $D_k$  denotes the  $k$ -th MPD or MRD discriminator submodules.  $\mathcal{L}_{adv}$  uses the least-square GAN [29] as follows:

$$\mathcal{L}_{adv}(G; D_k) = \mathbb{E}_s \left[ (D_k(G(s)) - 1)^2 \right], \quad \mathcal{L}_{adv}(D_k; G) = \mathbb{E}_{(x,s)} \left[ (D_k(x) - 1)^2 + (D_k(G(s)))^2 \right], \quad (2)$$

where  $x$  is the ground-truth waveform, and  $s$  is the input mel spectrogram. The feature matching loss  $\mathcal{L}_{fm}$  [23, 22] minimizes the  $\ell_1$  distance for every intermediate features from the discriminator layers:

$$\mathcal{L}_{fm}(G; D_k) = \mathbb{E}_{(x,s)} \left[ \sum_{i=1}^T \frac{1}{N} \|D_k^i(x) - D_k^i(G(s))\|_1 \right], \quad (3)$$

where  $T$  is the number of layers of the sub-discriminator  $D_k$ . The generator loss  $\mathcal{L}_G$  also has the spectral  $\ell_1$  regression loss between the mel spectrogram of the synthesized waveform and the corresponding ground-truth:

$$\mathcal{L}_{mel}(G) = \mathbb{E}_{(x,s)} \left[ \|\phi(x) - \phi(G(s))\|_1 \right], \quad (4)$$

where  $\phi$  is the STFT function that converts the waveform into the mel spectrogram. We used the scalar weights  $\lambda_{fm} = 2$  and  $\lambda_{mel} = 45$  identically as [19].

## C Practical Lessons for Large Scale GAN Training

In this section, we document additional directions that we have explored for improving the model architecture and large scale training, but resulted in worse perceptual quality from our preliminary study. We do not make conclusive claims based on these observations because the methods we explored here may have been ineffective specific to our BigVGAN settings. Nevertheless, we believe that reporting negative results can be helpful to future research endeavors [4].

**Anti-aliased upsampling layers** Our BigVGAN uses anti-aliased activation for AMP modules. We also explored replacing the transposed convolution-based upsampling layers, which are known to contain checkerboard aliasing [34], to the anti-aliased alternatives with different low-pass filter hyperparameters. However, this introduced significant instabilities during training, leading to early collapse even with the aforementioned stabilization. We also tried out nearest-neighbor upsampling which is reported to have less artifacts for audio synthesis [41], but it also resulted in the early collapse.

**Periodic discriminators** Inspired by the improvements with the periodic activation function to the generator, we experimented on discriminators with *Snake* function. However, it degraded the quality with the diverging feature matching loss [19] from the discriminators. We conjecture that the periodic activation to the discriminator is not stable enough to improve the gradient from the feature matching loss.

**Spectral normalization** Spectral normalization [31] is a widely adopted method to stabilize GAN training in image domain. We tried applying spectral normalization to all discriminator submodules and found that it can stabilize the training without the early divergence of the generator. However, it suffered from a significant degradation with the excessive amount of phase mismatch artifacts, similar to the findings in the previous work [22]. We found that the gradient from MPD is over-regularized and the generator start to solely rely on the mel regression loss. Because MPD is repeatedly found to be a key inductive bias for high-quality audio synthesis [19], regularizing MPD leads to worse result.

**Larger discriminators** We hypothesized that the enlarged generator can be slower to learn, thereby trivializing the discriminator in the early training (loss converge to zero). We tried to balance the training by enlarging the discriminators, such as employing more MPD sub-discriminators or enlarging the channel width of MPD and MRD modules. The large discriminator partially alleviated the early collapse, but the audio quality degraded in most cases, and showed no clear improvements even with our best configuration.

**Even larger generators** We experimented with deeper model with 8 upsampling blocks with ratio of [2, 2, 2, 2, 2, 2, 2, 2]. However, it exhibited high-frequency rattling artifacts and degraded the quality. We conjecture that generating fine-grained high-frequency details from the early upsampling blocks can be arbitrary [17] and unstable when using the filtered periodic nonlinearity. We also tried to further increase the number of convolution channels to 2048, but it suffered from early collapse.

**Data augmentation** Data augmentation is one of major methods that improve model generalization, which is also repeatedly found to be valuable in GAN literature [16]. We explored augmenting the data by applying SpecAugment [36] to the input mel spectrogram. However, SpecAugment resulted in over-smoothing artifacts in waveform, because it enforces the model to map multiple distorted mel spectrograms to the same waveform, which counters the upsampling process in generative models. We also tried applying mixup-like [61] approach to the waveform by using a convex combination of two audio samples and its corresponding mel spectrogram. However, this occasionally resulted in a mixed voice of two speaker identities during a single-speaker inference without noticeable improvement in perceptual quality.

**Positional encoding** Inspired by using partial autoregression [40, 32] to provide inductive bias of the cumulative sum relationship of pitch and phase [32], we explored whether we can provide an approximate inductive bias in a non-autoregressive manner by injecting a sinusoidal positional encoding [54] to the generator. However, the generator with positional encoding is only exposed to the fixed audio segment at training ( $\sim 0.3$  seconds with 8,192 time-steps) and unable to extrapolate unknown and significantly longer sequence at inference (e.g., several seconds).

## D Expanded Ablation Study and Comparison with Objective Evaluation

We perform additional ablation study and comparison to previous work with the automatic objective evaluation.

**Ablation study and objective results** Table 8 and 9 show the expanded objective results evaluated on LibriTTS, including the ablation models of BigVGAN-base, UnivNet [11], and SC-WaveRNN [37].

SC-WaveRNN [37] is a universal vocoder based on WaveRNN with a speaker embedding from a separately trained encoder network. We replicate the training procedure following [37] using the official implementation, while matching training data and audio hyperparameters used in this study (i.e., LibriTTS-full, 24,000Hz sampling rate and a 100-band log-mel spectrogram with full-band frequency). Although the model can generate speech with diverse speaker identities, we find that the performance is significantly worse than GAN vocoders both in objective scores and human listening test. It fails to generate intelligible audio for unseen recording environments and out-of-distribution sample. We conjecture that the speaker embedding network is not robust enough to generalize to such setups. We exclude SC-WaveRNN from the MOS and SMOS test because an exposure to the audio samples with poor quality can introduce listener’s bias and inflate the scores for other models.

Table 8: Objective results of BigVGAN from dev-clean of LibriTTS including ablation models of BigVGAN-base and previous work. †: pretrained weight obtained from an open-source repository which used train-clean-360 subset for training.

LibriTTS (clean)	MAE(↓)	M-STFT(↓)	PESQ(↑)	MCD(↓)	Periodicity(↓)	V/UV F1(↑)
SC-WaveRNN	0.4477	1.5658	1.927	1.0964	0.2056	0.9047
UnivNet-c32†	0.2803	0.9552	3.348	0.7017	0.1342	0.9433
UnivNet-c32	0.2772	0.9433	3.310	0.6942	0.1356	0.9435
HiFi-GAN (V1)	0.2579	0.9773	3.042	0.6257	0.1545	0.9306
BigVGAN-base	0.1629	0.8675	3.569	0.4429	0.1295	0.9453
w/o filter	0.1770	0.8838	3.472	0.4624	0.1354	0.9437
w/o filter & snake	0.1899	0.9047	3.351	0.4852	0.1399	0.9401
BigVGAN	<b>0.1101</b>	<b>0.8151</b>	<b>3.896</b>	<b>0.3591</b>	<b>0.1106</b>	<b>0.9564</b>

We also train UnivNet-c32 [11] on LibriTTS-full using the open-source implementation (note that UnivNet uses the 24,000Hz sampling rate and the 100-band log-mel spectrogram with full-band frequency by default). However, unlike the HiFi-GAN and BigVGAN architectures, using the large-scale dataset did not improve the quality of the UnivNet architecture. Overall, the publicly available model trained on train-clean-360 scores marginally better in terms of PESQ and periodicity error compared to our checkpoint trained on LibriTTS-full. Other metrics exhibit different preference depending on the training set. The subjective quality is indistinguishable between the two checkpoints, including the out-of-distribution setup. We conjecture that the UnivNet architecture is harder to generalize to the unseen recording environments. For subjective MOS and SMOS tests, we choose to use the publicly available checkpoint using train-clean-360 to faithfully represent the performance of the previous work. Note that the open-source implementation of UnivNet is unofficial. Therefore, our observation does not lead to the conclusion that UnivNet is worse than HiFi-GAN.

From both clean and other recording environments, BigVGAN-base showed consistent improvements in all metrics compared to its ablation models. Specifically, BigVGAN-base (without filter & snake) refers to the vanilla HiFi-GAN architecture trained with MRD replacing MSD. Similar to the findings in [11], MRD provides more accurate modeling of the waveform by sharpening the spectral structure. Applying *Snake* activation (BigVGAN-base without filter) increases accuracy and reduces the periodicity error from the desired inductive bias. Finally, incorporating the continuous feature representation and the low-pass filter (BigVGAN-base) provide the best accuracy by suppressing aliasing and high frequency artifacts. Our final 112M BigVGAN substantially improves the accuracy for the state-of-the-art universal neural vocoding.

**Additional unseen speech dataset** Table 10 and 11 show the objective speech evaluation metric results gathered from VCTK and LJSpeech dataset, consistent with the results from Table 8 and 9. Although the dataset is not included for training BigVGAN and the baseline HiFi-GAN, all GAN-based models performed comparatively well from our subjective listening test. This indicates that given diverse enough training data, modern non-autoregressive GAN vocoder can synthesize high-quality speech with unseen speaker identities from the clean recording environment.



Table 9: Objective results of BigVGAN from dev-other of LibriTTS including ablation models of BigVGAN-base and previous work. †: pretrained weight obtained from an open-source repository which used train-clean-360 subset for training.

LibriTTS (other)	MAE(↓)	M-STFT(↓)	PESQ(↑)	MCD(↓)	Periodicity(↓)	V/UV F1(↑)
SC-WaveRNN	0.5623	1.8338	1.729	1.5946	0.2526	0.8678
UnivNet-c32†	0.3027	0.9973	3.166	0.8643	0.1439	0.9345
UnivNet-c32	0.2998	0.9883	3.107	0.8495	0.1457	0.9337
HiFi-GAN (V1)	0.2724	1.026	2.853	0.6948	0.1585	0.9294
BigVGAN-base	0.1684	0.9052	3.502	0.4776	0.1357	0.9403
w/o filter	0.1844	0.9223	3.364	0.5017	0.1391	0.9395
w/o filter & snake	0.2008	0.9456	3.240	0.5389	0.1451	0.9344
BigVGAN	<b>0.1139</b>	<b>0.8517</b>	<b>3.825</b>	<b>0.3906</b>	<b>0.1218</b>	<b>0.9486</b>

Table 10: Objective results from unseen VCTK dataset. We used randomly selected 100 audio clips. †: pretrained weight obtained from an open-source repository which used train-clean-360 subset for training.

VCTK	MAE(↓)	M-STFT(↓)	PESQ(↑)	MCD(↓)	Periodicity(↓)	V/UV F1(↑)
SC-WaveRNN	0.6125	2.3274	1.576	1.4717	0.2174	0.8896
UnivNet-c32†	0.2753	0.9476	3.235	0.7180	0.1131	0.9535
UnivNet-c32	0.2820	0.9586	3.184	0.7403	0.1198	0.9434
HiFi-GAN (V1)	0.2541	0.9859	3.029	0.6795	0.1336	0.9375
BigVGAN-base	0.1613	0.8767	3.453	0.4602	0.1126	0.9529
w/o filter	0.1739	0.8935	3.379	0.4924	0.1128	0.9528
w/o filter & snake	0.1885	0.9184	3.316	0.5159	0.1208	0.9481
BigVGAN	<b>0.1104</b>	<b>0.8222</b>	<b>3.800</b>	<b>0.3884</b>	<b>0.0993</b>	<b>0.9578</b>

Table 11: Objective results from unseen LJSpeech dataset. We used randomly selected 100 audio clips. †: pretrained weight obtained from an open-source repository which used train-clean-360 subset for training.

LJSpeech	MAE(↓)	M-STFT(↓)	PESQ(↑)	MCD(↓)	Periodicity(↓)	V/UV F1(↑)
SC-WaveRNN	0.4936	1.7348	1.813	1.7387	0.1944	0.9207
UnivNet-c32†	0.3418	1.0613	3.425	1.1903	0.1210	0.9519
UnivNet-c32	0.3356	1.0429	3.384	1.1356	0.1230	0.9503
HiFi-GAN (V1)	0.3008	1.0950	3.210	1.7370	0.1347	0.9456
BigVGAN-base	0.1826	0.9228	3.695	<b>0.6956</b>	0.1152	0.9554
w/o filter	0.2015	0.9395	3.662	0.9715	0.1169	0.9548
w/o filter & snake	0.2263	0.9946	3.521	1.1320	0.1299	0.9479
BigVGAN	<b>0.1355</b>	<b>0.8921</b>	<b>4.050</b>	0.7790	<b>0.0983</b>	<b>0.9634</b>

## **E Ethical Considerations and Societal Impacts**

Our study, using BigVGAN, investigates the task of universal neural vocoding: synthesizing an accurate audio waveform conditioned on the corresponding mel spectrogram regardless of its characteristics, such as genders, speaker identities, languages, and recording environments. BigVGAN demonstrated a significant advancement of the generative modeling of audio with state-of-the-art performance using the large-scale LibriTTS speech corpus. As neural vocoder has been situated in a cornerstone method of human-computer interaction with practical impact, one should carefully assess the quality of the neural vocoder across diverse scenarios. Because LibriTTS only contains English speakers, our experimental design includes unseen languages at evaluation, in an effort to address such concern. Although we have not found an indication that BigVGAN’s performance is biased towards certain languages or speaker identities, we expect that an inclusion of more diverse languages and speakers in the training dataset would further eliminate the concern and reduce potential risks of social discrimination based on the quality of the synthesized waveform from BigVGAN.

While the state-of-the-art quality of universal neural vocoding from BigVGAN would foster numerous downstream applications, on a flip side, it can also increase a possibility of a malicious usage of the technology. For example, if it is applied to text-to-speech using real-world speech data from the web, the increased realism could be exploited as a personal attack such as synthesizing offensive utterance using the target’s voice. The unprecedented universal vocoding quality of BigVGAN calls for methods to prevent the potential negative societal impacts, such as protecting automatic speaker verification from the threat of spoofing attack, automatic detection of the synthesized voice from various downstream applications, and audio steganography or watermark technique that indicates the machine-generated audio.